Static and Cyclic Design Aspects for Foundation Piles of Offshore Wind Farms

Dr. Axel Nernheim
WTM Engineers GmbH, Hamburg, Germany
Andre Stang
THM - University of Applied Sciences, Giessen, Germany

GEOQuébec 2015
Challenges from North to South
Des défis du Nord au Sud

ABSTRACT
Part of the proposed transition of the German energy market to renewable energy will be based on the large-scale development of offshore wind farms. Due to large pile diameters and distinct cyclic loading effects from wind and waves, new challenges arise for the pile design of the foundations. This contribution gives an overview of the specific cyclic pile design aspects with a focus on offshore wind farm installations in the German sector of the North Sea. Three methods are presented: An interaction diagram, an analytical and a numerical approach.

RÉSUMÉ
Une part de la transition proposée, du marché allemand, de l'énergie vers les énergies renouvelables sera basée sur le développement à grande échelle de parcs éoliens en mer. En raison du grand diamètre des pieux, ainsi que des actions cycliques résultantes du vent et des vagues, de nouveaux défis sont apparus quant au dimensionnement des pieux de fondation. Le présent article donne un aperçu des aspects spécifiques d'un dimensionnement de pieux exposés aux actions cycliques, en focalisant sur l'installation des parcs éoliens dans le secteur allemand de la mer du Nord. Trois méthodes sont présentées: un diagramme d'interaction, une approche analytique et une approche numérique.

1 INTRODUCTION

During the large-scale development of offshore wind farms in the German sector of the North Sea the installation of approximately 6500 MW capacity is scheduled until the year 2020.

Different innovative foundation concepts are used depending on water depth, soil and environmental conditions as well as the electric capacity of the installed turbine. Monopile foundations currently dominate near-shore wind farms with water depths lower than approximately 20 m and/or medium size turbines whereas in areas with larger water depths and/or large scale turbine sizes (e.g. the 6 MW class) space frame structures like tripods, tripiles or jacket structures are the prevailing foundation type.

Due to large pile diameters (approximately 2.5 m for jacket piles and maximum 7 m to 8 m for monopiles), cyclic loading effects from wind and waves in combination with the relatively low self-weight of the structure and the pile installation in an offshore environment, novel challenges emerge for the pile design.

The predicted <u>static</u> pile capacity of open-ended large diameter tubular steel piles for space frame jacket foundation concepts in the North Sea with predominantly non-cohesive soil has not been verified by in-situ static pile load tests so far. Based on a representative pile geometry for a jacket foundation and generic non-cohesive soil profiles this contribution illustrates the variety of predicted static pile capacities using the widely used pure-empirical method from Germany as well as the design method of the API.

It has been documented previously that <u>cyclic</u> load has a negative effect on the static pile capacity in non-cohesive soils. However, it has been a challenge since to quantify the amount of the pile capacity degradation. This contribution presents new innovative German design methods allowing the computation of pile capacity degradation and pile displacement accumulation. A validation as well as a worked example utilizing easy-to-use interaction diagrams, the analytical Kirsch/Richter method and the numerical method of Thomas reveal major influence parameters and the outcome of the cyclic axial pile design of a jacket pile foundation in non-cohesive soil.

2 STATIC PILE CAPACITY

2.1 Introduction and overview

Axially loaded piles in predominately non-cohesive soil subjected to <u>compression</u> forces transfer the load partly by shear generated along the shaft and partly by normal stresses generated at the base of the pile. Piles subjected to <u>tension</u> resist the forces by shear along the shaft area of the pile. The mobilization of the shaft and the base capacity requires a specific pile displacement, where the shaft capacity is fully mobilized at a much smaller displacement (typically 0.5% to 2% of the pile diameter) than the base capacity (typically 5% to 10% of the pile diameter) according to Fleming et. al. (2009).

In case of an open-ended pipe piles the pile inner shaft area may be included in the computation of shaft capacity in both, the tension and the compression design. However, open-ended pipe piles with rather small diameter plug either during driving or due to static loading in which case determination of the soil plug resistance is required. Eventually, the soil plug resistance depends on the degree of plugging. The evaluation of the plug occurrence can follow different approaches. A plug length ratio (PLR) is introduced in Yu and Yang (2012) which is implemented in the HKU-Method computing the base capacity of open-ended steel pipe piles in sand. The PLR is similar to the incremental filling ratio (IFR) that is implemented in the UWA-05 method computing the capacity of an axial loaded driven piles in sand. The PLR and the IFR should be estimated using eq. [1] and [2].

$$\mathrm{PLR} = (\mathrm{D_i}[\mathrm{cm}]/100)^{0.15} \qquad [1]$$

$$\mathrm{IFR} = \min\left[1, \left(\frac{\mathrm{D_i}[\mathrm{m}]}{1.5}\right)^{0.2}\right] \qquad [2]$$

Figure 1 shows that according to the PLR and IFR large diameter pipe piles with inner pile diameters $D_i \geq 1.5$m are loaded unplugged.

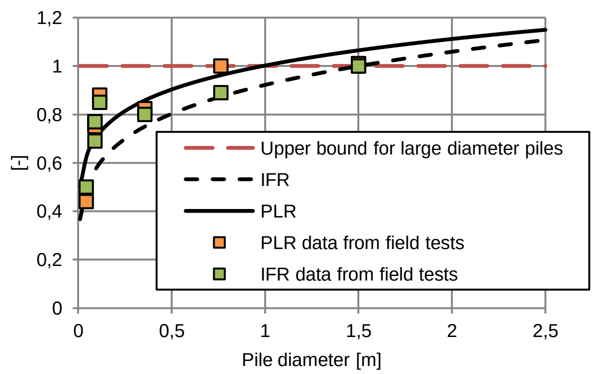

Figure 1. Proposal of the plugging evaluation using the IFR and the PLR with field test data from Yu and Yang (2012).

Hence, the calculation of compression and tension pile capacity of large diameter offshore piles should imply explicit consideration of the inner shaft friction:

$$\mathrm{R_{com}} = \mathrm{R_b} + \mathrm{R_{s,o}} + \mathrm{R_{s,i}} \qquad [3]$$

$$\mathrm{R_{ten}} = \mathrm{R_{s,o}} + \min\,[\mathrm{R_{s,i}}; \mathrm{W_{soil}}] \qquad [4]$$

Where

R_{com}	[kN]	Pile compression capacity
R_{ten}	[kN]	Pile tension capacity
R_b	[kN]	Base resistance
$R_{s,o}$	[kN]	Outer skin friction
$R_{s,i}$	[kN]	Inner skin friction
W_{soil}	[kN]	Weight of the inner soil column

In Germany the pile capacity estimation follows the widely used recommendations on piling of the German geotechnical society in EA-Pfaehle (2012) with the static design method which shall be introduced here as the EAP method. The Federal Maritime and Hydrographic Agency in Germany also accepts international standards such as the API RP 2A. The effective stress approach (β-method) for pile capacity prediction introduced in the main text of the API RP 2A is a widely accepted and used design method in offshore foundation engineering. In the commentary the API RP 2A also introduces the direct CPT q_c methods ICP-05, UWA-05, Fugro-05 and NGI-05, which have shown statistically better reliability in predicting the pile capacity in comparison to the β-method. However, experience using these methods applied on large diameter offshore piles is either limited or non-existing according to the API. Hence, these methods are neglected in this contribution.

2.2 Static design according to API

The compression unit shaft resistance can be computed from:

$$\tau_f = K_f \cdot \tan(\delta_{cv}) \cdot \sigma'_{v0} = \beta \cdot \sigma'_{v0} \leq \tau_{f,lim} \qquad [5]$$

The unit end bearing is calculated from:

$$q_b = N_q \cdot \sigma'_{v0} \leq q_{b,lim} \qquad [6]$$

Where

K_f	[-]	Coefficient of lateral earth pressure Plugged piles: $K_f = 1.0$ Unplugged piles: $K_f = 0.8$
δ_{cv}	[°]	Interface friction angle
σ'_{v0}	[kPa]	Effective vertical stresses
N_q	[-]	Dimensionless bearing capacity factor

For unplugged piles the inner shaft is considered equal the outer shaft friction. For fully plugged piles the unit end bearing acts over the entire pile tip gross area, otherwise over the pile annular area. The final total capacity is the minimum of plugged and unplugged pile capacity. According to GL-Wind (2005) tension shaft friction should be reduced to 2/3. Based on the idea that for long piles neither unit shaft friction τ_f nor unit end bearing q_b increase linearly with the overburden pressure σ'_{v0} the limit values $\tau_{f,lim}$ and $q_{b,lim}$ can be found in API RP 2A, chapter 6.4.3.

2.3 Static design according to German guidelines

The EAP method is a pure empirical method for driven piles in sand. Table 1 and Table 2 show empirical upper and lower unit end bearing and unit shaft friction for the measured CPT tip resistance, respectively.

Table 1: Unit end bearing q_b for driven reinforced and pre-stressed concrete piles in non-cohesive soils.

Normalized pile tip displacement s/D	Unit end bearing resistance q_b [MPa]		
	Averaged CPT q_c values [MPa]		
	7.5	15	25
0.035	2.2 – 5.0	4.0 – 6.5	4.5 – 7.5
0.1	4.2 – 6.0	7.6 – 10.2	8.75 – 11.5

Table 2: Unit shaft friction τ_f for driven reinforced and pre-stressed concrete piles in non-cohesive soils.

Pile tip displacement	Shaft resistance τ_f [kPa]		
	Averaged CPT q_c values [MPa]		
	7.5	15	25
S_{sg}	30 – 40	65 – 90	85 – 120
$S_{sg} = S_g = 0.1 \cdot D$	40 – 60	95 – 125	125 – 160

With

$$s_{sg}\ [\mathrm{cm}] = 0.5 \cdot R_s(s_{sg})\ [\mathrm{MN}] \leq 1.0\ [\mathrm{cm}] \quad [7]$$

Where

s_{sg}	[cm]	Required displacement to activate full shaft resistance
s_g	[cm]	Limit displacement of driven piles; typically ($s_g = 0.1 \cdot D$).

For steel pipe piles the values in Table 1 and Table 2 have to be multiplied by the adaption factors $\boldsymbol{\eta_b}$ and $\boldsymbol{\eta_s}$ (Figure 2). The EAP method does not consider inner shaft friction explicitly. The inner shaft friction is implicitly considered in the pile base capacity, which is why the pile base capacity is calculated using the pile tip gross area.

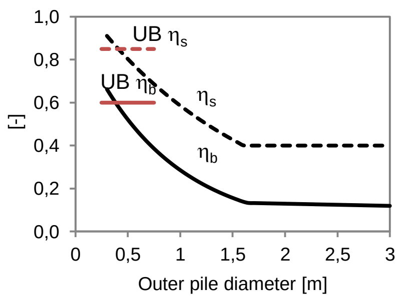

Figure 2: Adaption factors for base $\boldsymbol{\eta_b}$ and shaft resistance $\boldsymbol{\eta_s}$ according to Lueking (2010) and upper bound (UB) values according to EA-Pfaehle (2012).

2.4 Example of an offshore pile

The CPT q_c in Figure 3 illustrates a generic location with predominately very dense sand, which is typical for the north sea. The geometry of an offshore large diameter pile for a jacket foundation is listed below:

- Pile outer diameter D_o = 2.44 [m]
- Pile wall thickness t_w = 50 [mm]
- Pile embedded length L = 34 [m]

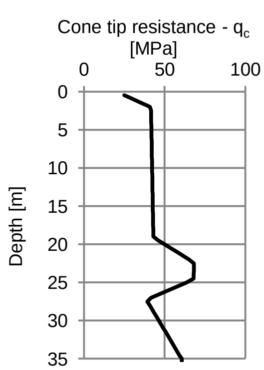

Figure 3: CPT q_c of a generic location in the north sea.

The computed compression pile capacity is illustrated in Figure **4**. For the sake of comparison the inner shaft friction in the API method has been allocated to the base capacity in Figure **4**, since the EAP method does not consider inner shaft friction explicitly. Average values are used for unit end bearing and shaft resistance according to Table **1** and Table **2**.

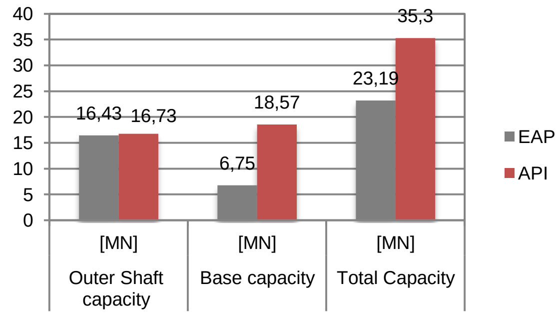

Figure 4: Pile capacity of the generic offshore location.

The deviation of the calculated total pile capacity can partly be attributed to the neglect of the inner shaft friction in the EAP method. This is considered as a disadvantage of the German method, since the plugging criteria in section 2.1 show that inner shaft friction can be considered explicitly. Eventually, the EAP method has recently been updated in Moormann and Kempfert (2014) introducing a new failure mechanism model for open-ended pipe piles with $D_o \geq 1.5\ \mathrm{m}$ with explicit consideration of the inner shaft friction. However, it is stated that due to a lack of experience and test data this model is currently not applicable to foundations of offshore wind turbines without project specific considerations.

3 CYCLIC PILE CAPACITY

3.1 Cyclic loading aspects

Due to cyclic loading changes in the soil grain structure an accumulation of pile displacement may be expected. Most literature sources dealing with post-cyclic pile capacity outline a degradation of shaft friction leading to a reduction of pile capacity.

According to API 2007 the pile shaft friction capacity is influenced by:

- Pile properties (embedment length, diameter, material)
- Soil characteristics (soil type, relative density, cyclic behaviour)
- Cyclic loading (type of load, load amplitude, number of load reversals).

The permitting authority for offshore wind farms in Germany, the BSH (Federal Maritime and Hydrographic Agency), requires the specific consideration of cyclic loads in the pile design process. Cyclic laboratory tests are recommended for a better prediction of the pile capacity.

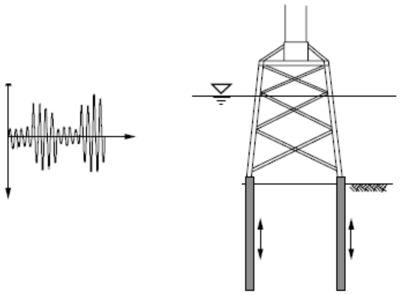

Figure 5. Example of a jacket pile foundation subjected to cyclic loading (Thomas 2011)

Offshore wind farm jacket structures are relatively lightweight structures subjected to large horizontal loads originating from sea motion waves and the operation of the wind turbine. Hence, cyclic load components act on the foundation piles of the jacket (Figure 5). These are characterized by the cyclic load amplitude, $\mathbf{F_{cyc}}$, the medium load level, $\mathbf{F_{mit}}$, and the number of load cycles, **N**.

The cyclic load is defined as swell load if the load remains either in tension or compression. Contrary, the alternating load implies a relatively low medium load level with the cyclic load amplitude causeing tension and compression forces at each load cycle (Figure 6).

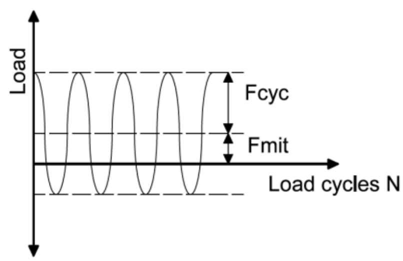

Figure 6. Cyclic medium load and load amplitude as a function of number of load cycles.

Axial cyclic loads acting on the pile head in a time-load history (Figure 5) are the result of a numerical modelling of the structure with statistically determined wind and wave actions. This has to be simplified into a multi-stage loading profile with corresponding load amplitudes, medium loads and load cycle numbers using a counting algorithm like the rainflow method. Finally, this is transformed into an equivalent one-stage loading profile causing the same reduction of pile capacity as the multi-stage profile (Figure 6).

3.2 Soil behaviour under cyclic loading

Changes of soil characteristics due to cyclic loading can be assessed by cyclic laboratory tests. Cyclic triaxial tests, resonant-column (RC) tests and cyclic simple shear tests are mentioned in BSH 2012.

Kirsch (2014) presents results of a cyclic simple shear test that describes non-cohesive soil behaviour when subjected to alternating loading and swell loading with various number of load cycles. Thus, either soil densification or dilation of the soil can be expected. However, alternating loads seem to influence the soil characteristics more significantly than swell loads.

3.3 Pile behaviour under cyclic loading

The behaviour of a pile subjected to cyclic loading is characterized by an accumulation of pile displacement (SLS) and by either an increase or decrease of shaft friction capacity (ULS).

According to Thomas and Kempfert (2013) the possible types of pile displacement accumulation due to different types of cyclic loading can be grouped in four categories (Figure 7). The shear strain generated by the cyclic pile displacement influences the grain structure of the soil surrounding the pile causing either shear strengthening or shear weakening of the soil, resulting in an increase or decrease of the shaft friction capacity, respectively.

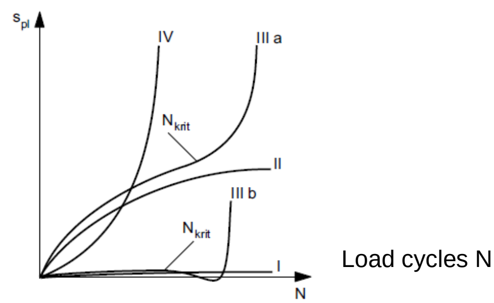

Figure 7. Illustration of possible accumulation of plastic pile displacements (Thomas and Kempfert 2013)

Respective load combinations of medium load level (x-axis) and cyclic amplitude (y-axis) referenced to the static ultimate pile capacity, R_{ult}, are shown in Figure 8. As described in Section 3.2, swell loads seem to have a softer behaviour than alternating loads with a lower risk of sudden displacement increases after a specific number of load cycles (Category II). Figure 8 also illustrates that the pile does not necessarily loose shaft friction due to cyclic loading (Category I): The threshold cyclic load level where no shaft degradation can be expected is often defined by 10 % to 20 %

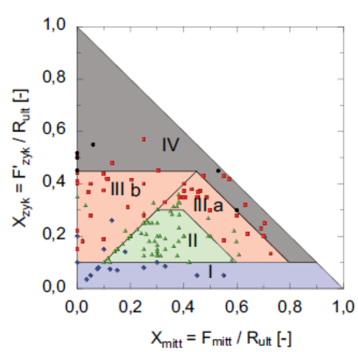

Figure 8. Interaction diagram showing possible pile displacement accumulation as a combination of cyclic and medium load level ($F'_{zyk} = F_{cyc}$) (Thomas and Kempfert 2013).

4 CYCLIC DESIGN METHODS

4.1 Introduction

A large number of documented cyclic axial pile load tests have demonstrated that the pile load behaviour can be significantly influenced by load amplitudes F_{cyc} larger than approximately 10 % of the ultimate pile capacity R_{ult}. For a more detailed estimation of these cases, the following steps should be considered in the cyclic design:

a. Static pile capacity R_{ult} e.g. based on methods described in section 2.3 and 2.4.
b. Cyclic accumulation of displacements s_{cyc}: Serviceability Limit State (SLS) verification
c. Post-cyclic pile capacity $R_{ult}(N)$ based on a cyclic shaft friction degradation: Ultimate Limit State (ULS) verification

The cyclic design methods described below can either be used to estimate the ULS and/or the SLS pile behaviour.

4.2 Interaction diagram

Interaction diagrams allow a quick estimation of the shaft friction degradation due to cyclic load. Cyclic design parameters apart from the cyclic load and the number of load cycles are not required for this method. The cyclic and the medium load level define the y- and the x-axis, respectively. The diagonal in each interaction diagram defines the static boundary line. This line drops with the increase of load cycle numbers depicting the pile capacity degradation. In Kirsch et. al. (2011) a new interaction diagram is introduced that incorporates previous work on cyclic pile behaviour and that especially was developed to enable an appropriate consideration of cyclic loads with high amplitudes but low number of cycles (Figure **9**).

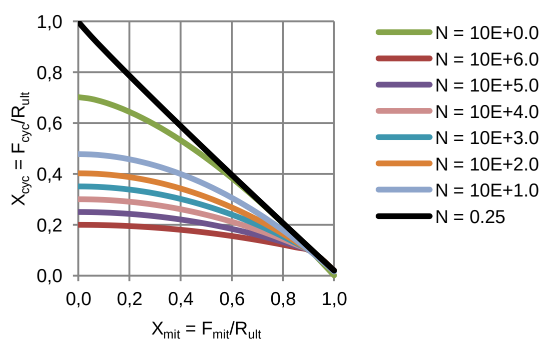

Figure 9. Kirsch/Richter/Mittag interaction diagram (Kirsch et. al. 2011).

The pile capacity degradation is computed using an utilisation factor μ_k multiplied by the maximum pile capacity degradation $\Delta R_{cyc,max}$, which can be calculated from the equation [8].

$$\Delta R_{cyc}(N) = \mu \cdot \Delta R_{cyc,max} \quad [8]$$

Where

$$\mu = \frac{L_1}{L_1 + L_2} \quad [9]$$

$$\Delta R_{cyc,max} = \frac{L_3}{L_1 + L_2 + L_3} \cdot R_{ult} \quad [10]$$

Both, the calculation of the maximum pile capacity degradation (eq. [10]) and the calculation of the utilisation factor (eq. [9]) require the determination of the segments L1, L2 and L3 (Figure 10).

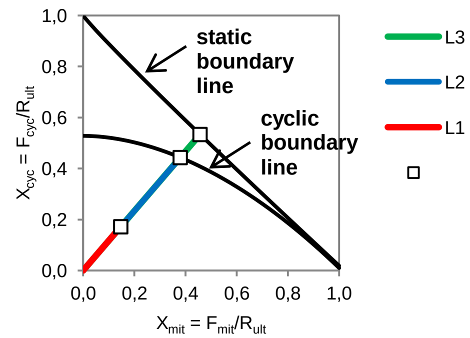

Figure 10. Definition of the segments L1, L2 and L3 in the Kirsch/Richter/Mittag interaction diagram.

The cyclic and medium load level defines the segment L1. The determination of segment L2 requires the cyclic boundary line, which is a function of N and can be calculated from:

$$X_{cyc} = \kappa \cdot \left(1 - 1.11^{EXP} \cdot X_{mit}^{EXP}\right) + 0.1235 \cdot X_{mit}^{EXP} \quad [11]$$

Where

$$\kappa = 0.5 + 0.67 \cdot [\log(N+1) - 1.0746 \cdot \log(N)] \quad [12]$$

$$EXP = 1 - 1.5 \cdot [\log(N+1) - \log(N)] \quad [13]$$

Eventually, Figure 10 illustrates that the intersection of the extended linear function defined by segment L1 and the static and cyclic boundary line define the segments L2 and L3.

4.3 Analytical method according to Kirsch/Richter

A method to approximate both the pile capacity degradation and the accumulation of pile displacement due to cyclic loading is introduced in Kirsch and Richter (2011). The method enables the computation of the shaft friction degradation due to cyclic compaction of the surrounding soil as a result of cyclic shear and the computation of axial deformations due to an accumulation of cyclic shear strain.

The unit shaft friction degradation due to cyclic soil compaction can be calculated from:

$$\Delta\tau(N) = 2G_w \cdot \tan(\delta_{mob}) \cdot \Delta D^* \cdot \left[\gamma_{cyc} \cdot \left(\frac{\gamma_{cyc}}{\gamma_{grenz}} - 1\right) - 0.5 \cdot \alpha \cdot \gamma_{grenz}\left(\frac{\gamma_{cyc}^2}{\gamma_{grenz}^2} - 1\right)\right] \quad [14]$$

With

$$\Delta D^* = 0.5 \cdot I_D^{-2.32} \cdot \log_{10}(N+1) \quad [15]$$

$$\gamma_{cyc} = \frac{\tau_{cyc}}{G_{cyc}} = \frac{F_{cyc}}{A_{shaft} \cdot G_{cyc}} \quad [16]$$

Where

I_D	[-]	Soil relative density
N	[-]	Number of load cycles
G_w	[MPa]	Shear modulus for reversed load
δ_{mob}	[°]	Mobilized interface friction angle
δ_{cv}	[°]	Interface friction angle
$R_{s,k}$	[MN]	Characteristic static shaft friction resistance ($Q_s = R_{s,k}$)
$\Delta\tau(N)$	[kPa]	Unit shaft friction degradation
G_{cyc}	[Mpa]	Cyclic shear modulus
α	[-]	Dilation parameter
γ_{cyc}	[-]	Cyclic shear strain
γ_{grenz}	[-]	Threshold cyclic shear strain

The product of the unit shaft friction and the pile shaft area yields the pile capacity degradation due to cyclic load:

$$\Delta R_{cyc}(N) = \Delta\tau(N) \cdot A_{shaft} \quad [17]$$

The cyclic pile displacement accumulations can be calculated from:

$$S_{cyc} = (1\Delta\gamma + 2\Delta\gamma_{cyc}) \cdot r_0 \cdot \ln\left(\frac{r_m}{r_0}\right) \quad [18]$$

With

$$r_m = 2.5 \cdot L \cdot (1-\nu) \quad [19]$$

Where

L	[m]	Pile length
r_0	[m]	Pile radius
ν	[-]	Soil poisson's ratio

The total cyclic pile displacement is the sum of the cyclic strain due to soil compaction $1\Delta\gamma$ (eq. [17]) and due to cyclic creep $2\Delta\gamma_{cyc}$ (eq. [21]).

$$1\Delta\gamma = \left(\frac{\kappa_2}{1-\kappa_2/c_1} - \frac{\kappa_1}{1-\kappa_1/c_1}\right) \cdot \gamma_r \quad [17]$$

With the pre- and post-cyclic load level κ_1 and κ_2, respectively:

$$\kappa_1 = (\tau_{cyc} + \tau_{mit})/\tau_{ult} \quad [18]$$

$$\kappa_2 = (\tau_{cyc} + \tau_{mit})/(\tau_{ult} - \Delta\tau(N)) \quad [19]$$

The cyclic creep for the first load cycle is calculated from:

$$2\Delta\gamma = \left(\frac{\kappa_1}{1-\kappa_1/c_2} - \frac{\kappa_1}{1-\kappa_1/c_2}\right) \cdot \gamma_r \quad [20]$$

For all following cycles the cyclic creep can be calculated from:

$$2\Delta\gamma_{cyc} = 2\Delta\gamma \cdot [1 + \zeta \cdot \ln(N)] \quad [21]$$

Where

ζ	[-]	Factor for cyclic creep
γ_r	[-]	Reference shear strain
N	[-]	Number of load cycles
G_w	[MPa]	Shear modulus for reversed load
c	[-]	Factor describing the hysteresis curvature for the first cycle c_1 and the following cycles c_2.

The theory background as well as a detailed derivation of the equations can be found in Kirsch and Richter (2011).

4.4 ZYKLAX method

The ZYKLAX method is based on the computation of the pile response with a load transfer approach using theoretically derived t-z and Q-z-curves. For estimation of the cyclic pile response the method requires a one stage loading profile. The approach has been calibrated using a large number of laboratory and in-situ static and cyclic axial pile load tests. Details are described in Thomas (2011) and Thomas and Kempfert (2013).

For the static part, established approaches for the pile skin and the pile tip are used to describe the non-linear behaviour of the pile. These analytical approaches are based on the one-dimensional spring approach as a load-transfer mechanism.

According to Thomas (2011) the static pile displacement s_s of the pile skin can be calculated from:

$$s_s = \frac{\tau_0 \cdot r_0}{G_0 \cdot g_s} \cdot \ln\left(\frac{\left(\frac{r_m}{r_0}\right)^{g_s} - R_{fs} \cdot \left(\frac{\tau_0}{\tau_{ult}}\right)^{g_s}}{1 - R_{fs} \cdot \left(\frac{\tau_0}{\tau_{ult}}\right)^{g_s}}\right) \quad [22]$$

Where

τ_0	[kPa]	Shear stress at pile skin
τ_{ult}	[kPa]	Shear stress under ultimate loading conditions
G_0	[kPa]	Soil shear modulus at small strains
r_0	[m]	Pile radius
r_m	[m]	Pile influence radius
R_f	[-]	Empirical model parameter
g_s	[-]	Empirical model parameter

and the static pile base displacement s_b:

$$s_b = \frac{R_b \cdot (1-\nu)}{4 \cdot G_0 \cdot r_0 \cdot \left(1 - R_{fb} \cdot \left(\frac{R_b}{R_{b,ult}}\right)^{g_s}\right)} \qquad [23]$$

Where

R_b	[kN]	Pile base resistance
$R_{b,ult}$	[kN]	Ultimate pile base resistance
ν	[-]	Poisson ratio

For the cyclic part, the static model has been extended based on test results to describe the cyclic behaviour of the pile skin.

The displacement $s_{s,W}(N)$ of pile skin due to loading/reloading in cycle N can be calculated from:

$$\begin{aligned} s_{s,W}(N) &= s_{min} + \frac{(\tau_0 - \tau_{min}) \cdot r_0}{G_0 \cdot g_s} \\ &\cdot \ln\left(\frac{\left(\frac{r_m}{r_0}\right)^{g_s} - R_{fs} \cdot \left(\frac{|\tau_0 - \tau_{min}|}{\kappa \cdot \delta_N \cdot \beta_N \cdot \tau_{ult}}\right)^{g_s}}{1 - R_{fs} \cdot \left(\frac{|\tau_0 - \tau_{min}|}{\kappa \cdot \delta_N \cdot \beta_N \cdot \tau_{ult}}\right)^{g_s}}\right) \end{aligned} \qquad [24]$$

Where

s_{min}	[mm]	Displacement of pile skin at begin reloading
τ_{min}	[kPa]	Shear stress at begin of reloading
β_N	[-]	Model parameter describing adaption of pile capacity
δ_n	[-]	Model parameter: Accumulation of plastic displacement

and the displacement $s_{s,E}(N)$ of pile skin due to unloading in cycle N:

$$\begin{aligned} s_{s,E}(N) &= s_{max} + \frac{(\tau_0 - \tau_{max}) \cdot r_0}{G_0 \cdot g_s} \\ &\cdot \ln\left(\frac{\left(\frac{r_m}{r_0}\right)^{g_s} - R_{fs} \cdot \left(\frac{|\tau_0 - \tau_{max}|}{\kappa \cdot \beta_N \cdot \tau_{ult}}\right)^{g_s}}{1 - R_{fs} \cdot \left(\frac{|\tau_0 - \tau_{max}|}{\kappa \cdot \beta_N \cdot \tau_{ult}}\right)^{g_s}}\right) \end{aligned} \qquad [25]$$

Where

s_{max}	[mm]	Displacement of pile skin at begin unloading
τ_{max}	[kPa]	Shear stress at begin of unloading
κ	[-]	Model parameter: Shape of hysteresis

The interaction of above described pile tip and skin behaviour is implemented in a numerical approach. With this approach multiple soil layers can also be modelled.

The concept for calculation of post-cyclic pile capacity is not included here for brevity, reference is made to Thomas 2011.

4.5 RATZ

The internationally established program RATZ has a built-in algorithm to model the degradation of shaft capacity and pile displacement accumulation due to cyclic loading. The program is based on a load transfer approach using empirically derived t-z- and Q-z-curves. The exact shape of these curves depends on the peak shaft friction from static analysis and on design soil parameters that should be derived from laboratory tests.

In Seidel and Coronel (2011) the RATZ program has been proven being appropriate for cyclic pile response analysis since cyclic field tests have been back calculated with adequate conformity.

Since the focus of this contribution lies explicitly on German methods for cyclic pile response analysis the RATZ program will not be discussed further. However, a detailed description of the theory background can be found in Randolph and Gourvenec (2011) and Seidel and Coronel (2011).

5 VALIDATION WITH PILE LOAD TEST

5.1 General

A number of static and cyclic in-situ pile load tests have been performed at the Dunkirk test site as part of the GOPAL (Grouted Offshore Piles for Alternating Loading) research project. The test program and results are described in Jardine & Standing (2000). The soil conditions (below an upper layer of sand fill) in the upper 30 m consist of Flandrian Sand, which is marine sand of varying density. The CPT profile at the test location R3 is presented in Figure Figure 11.

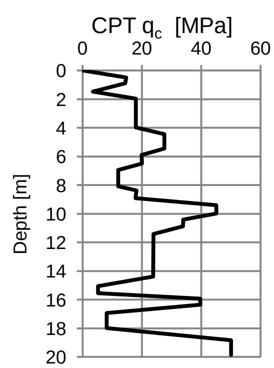

Figure 11. CPT q_c of the pile R3 from Jardine and Standing (2000).

Pile R3 is selected in this paper for validation purposes, the most relevant geometry data is summarized below:

- Pile outer diameter D_o = 0.457 [m]
- Pile wall thickness:
  - upper pile (2.5m) t_w = 20 [mm]
  - lower pile (18m) t_w = 13.5 [mm]
- Pile embedded length L = 34 [m]

Loading is applied in a multi-stage tension loading history: First, a slow static maintained loading test (R3.T1) is carried out up to a maximum applied load of 2000 kN at a pile head displacement of 10.3 mm followed by a cyclic loading test (R3.CY2) with a swell load of 0 to 1400 kN and a permanent head displacement of 6.8 mm after N = 200 cycles applied:

- Cyclic load amplitude F_{cyc} = 700 [kN]
- Medium load F_{mit} = 700 [kN]
- Number of load cycles N = 200 [-]

The static load test was terminated before reaching the ultimate pile capacity, but according to Jardine & Standing (2000) an ultimate capacity of 2320 kN has been estimated. Hence, a maximum load level of 60 % of the static pile capacity has been applied during the cyclic load test.

5.2 Back calculation of cyclic load test

The pile displacement accumulation of the cyclic load test R3.CY2 as well as results using the methods described above are presented in Figure 12.The ZYKLAX and the RATZ programs are capable of modelling the hysteresis of each load cycle. Therefore, Figure 12 shows displacements for the maximum and the minimum displacement of each load cycle. Contrary, the Kirsch/Richter method yields maximum values for cyclic pile displacement only.

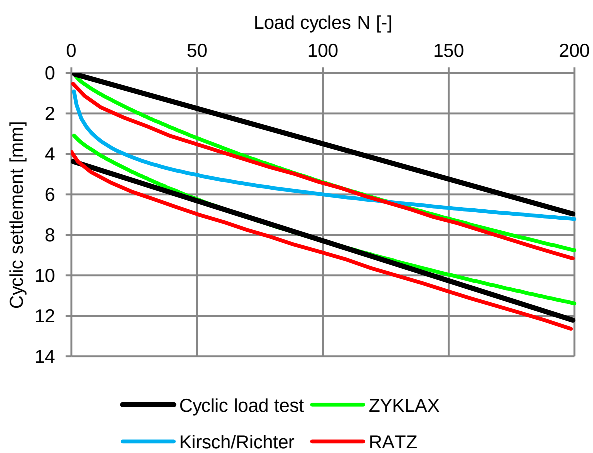

Figure 12. Comparison of cyclic pile displacement from ZYKLAX, RATZ and Kirsch/Richter with cyclic load test data.

In Figure 12 the maximum and minimum cyclic displacements of ZYKLAX show adequate conformity with the cyclic load test and also with the RATZ results. The results of the Kirsch/Richter method display deviation in terms of the shape of the displacement curve and in terms of the final pile settlement after 200 load cycles, but the computed displacements remain in the range of minimum and maximum displacements of the test data. Generally, the results of all methods show adequate conformity with the measured loading history proving their capability for cyclic response analysis.

Eventually, the conformity with the load test results could only have been achieved by adopting the design parameters in both methods. Therefore, to enable best performance of the Kirsch/Richter and the ZYKLAX methods, input parameters, such as the initial pile capacity and further cyclic design parameters have to be selected carefully and should preferentially be derived from cyclic laboratory tests.

6 EXAMPLE OF AN OFFSHORE FOUNDATION

6.1 General

This worked example summarises the cyclic pile response analysis of a large diameter offshore pile using an interaction diagram (section 4.2), the Kirsch/Richter method (section 4.3) and the ZYKLAX method (section 4.4).

A generic location with a typical CPT q_c profile of North Sea soil conditions is illustrated in Figure 3. Utilising the API design method and the pile geometry from section 2.4 the compression and tension shaft friction is 35.3 MN and 16.73 MN, respectively.

It is assumed that the pile is subjected to a tension cyclic swell load. The cyclic load components are listed in Table **3** comprising Load case A and B which fall into the load category I and II in Figure 7 and Figure 8. A number of N = 1000 load cycles is selected for demonstration purposes.

Table 3: Cyclic load components and cyclic medium load levels used in the worked example.

Load case	F_{cyc} [kN]	F_{mit} [kN]	N [-]	X_{cyc} [-]	X_{med} [-]
LC A	1673	1673	1000	0.10	0.10
LC B	3346	4182.5	1000	0.20	0.25

The selected static and cyclic parameters used in the ZYKLAX method are summarised below:

G_0	=	95000	[kPa]	Average over pile
τ_{ult}	=	54	[kPa]	Average over pile
R_{fs}	=	0.995	[-]	
g_s	=	0.02	[-]	
κ	=	2.0	[-]	

The selected static and cyclic parameters used in the Kirsch/Richter method are summarised below:

I_D	=	0.75	[-]	c_1	=	1	[-]
e	=	0.51	[-]	c_2	=	1	[-]
α	=	0.25	[-]	ζ	=	2	[-]
γ_{grenz}	=	0.0002	[-]	ν	=	0.35	[-]
G_{cyc}	=	$0.4 \cdot G_{max}$	[MPa]				
G_w	=	$0.2 \cdot G_{max}$	[MPa]				

The cyclic response analysis comprises the calculation of the pile displacement as a function of the load cycles using ZYKLAX and the Kirsch/Richter method (section 6.2) as well the calculation of the degraded pile capacity using the Kirsch/Richter method and the interaction diagram (section 6.3).

6.2 Cyclic displacement

The cyclic pile displacement accumulation of the pile subjected to the cyclic load according to Table **3** is illustrated in Figure **13**. The ZYKLAX method is capable of modelling the hysteresis of each load cycle. Therefore Figure **13** shows displacements for the maximum and the minimum load of each load cycle. Contrary, the Kirsch/Richter method yields maximum displacements of each load cycle only.

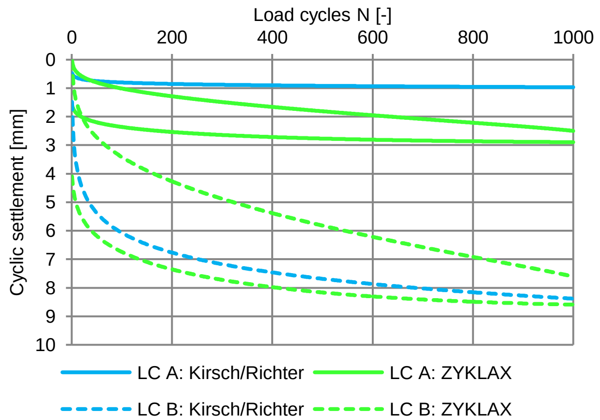

Figure 13. Comparison of cyclic pile displacement accumulation according to Kirsch/Richter and ZYKLAX.

Figure **13** shows that the marginal accumulation of pile displacements due to load case A using the Kirsch/Richter method and the ZYKLAX method corresponds to the expected pile displacement behaviour of category 1 according to Figure 7. Load case B influences cyclic pile behaviour more significantly. Eventually, the cyclic pile behaviour of the offshore pile subjected to this load case is in agreement with the pile displacement behaviour of category II from Figure 7. Due to the large number of specific static and cyclic input parameters to be selected for both methods, a careful selection of these values is essential for a correct displacement prediction. Figure **14** illustrates this necessity exemplarily for a variation of the ZYKLAX parameter κ in its documented range of values.

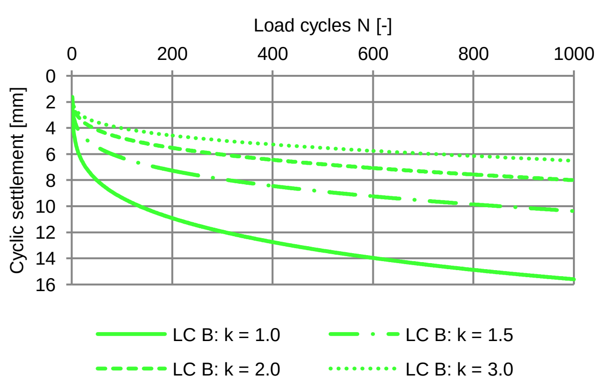

Figure 14. Sensitivity study adapting parameter κ using the ZYKLAX method for LC B.

These results indicate that as long as cyclic parameters have been chosen correctly these methods are in general applicable for offshore cyclic pile design.

6.3 Post-cyclic pile capacity

The post-cyclic pile capacity has been estimated using the Kirsch/Richter method and the interaction diagram of Kirsch/Richter/Mittag. The results for load cases A and B are summarised in Table **4**.

Table 4: Pile capacity degradation according to the Kirsch/Richter method and the interaction diagram of Kirsch/Richter/Mittag.

Load case (LC)		$\Delta R_{cyc}(N)$			
		Kirsch/Richter		Interaction diagram	
		[%]	[kN]	[%]	[kN]
A	N=10	0.0	0.0	5,83	811
	N=100	0.0	0.0	9,6	1332
	N=1000	0.0	0.0	13.4	1871
B	N=10	0,62	104	10.1	1403
	N=100	1,21	202	16.9	2367
	N=1000	1.78	297	24.3	3382

The dimensions of the pile capacity degradation vary significantly for both load cases.

For low amplitudes (LC A) the Kirsch/Richter method predicts no pile capacity degradation, whereas the interaction diagram predicts a degradation between 5% and 14% for low and high numbers of load cycles, respectively. Comparing the results with the computed cyclic pile displacement, which show marginal pile displacement in the range of 3 mm only, the large amount of pile capacity degradation predicted by the interaction diagrams appears unreasonable.

For larger amplitudes (LC B) the deviation in predicted degradation remains significant. The estimated degradation of the interaction diagrams ranges between 10% and 25% for low and high number of cycles, respectively. Contrary, the estimated shaft friction degradation according to Kirsch/Richter lies between 0% and 2% only. Considering the cyclic pile displacement of 1 cm for this load case (Figure **13**) this degradation appears to be more reasonable.

In Kirsch and Richter (2012) the pile capacity degradation according to the Kirsch/Richter method, the Kirsch/Richter/Mittag interaction diagram and the RATZ program have been compared and similar results have been produced. The significant deviation between the Kirsch/Richter method and the interaction diagram highlights the importance of further research in this field.

7 SUMMARY AND CONCLUSIONS

Part of the challenge in the design of offshore wind farms is the distinct cyclic loading acting on the structure and the foundation due to wind and wave action. Three German methods to estimate the pile behavior under cyclic loading (development of displacements with load cycles) as well as the post-cyclic pile capacity (ultimate pile capacity under consideration of skin friction degradation) are presented. Due to the lack of in-situ tests with typical large offshore pile diameters, these methods are based on theoretical considerations as well as smaller diameter in-situ or laboratory tests. A cyclic loading test of the Dunkirk test site has been used for a method-specific validation of parameters and to verify that the methods are applicable.

In a worked example of a typical offshore foundation the development of displacements s_{cyc} under cyclic loading (SLS) as well as the reduction of post-cyclic pile capacity ΔR_{ult} due to skin friction degradation (ULS) is presented. This capacity reduction typically leads to pile extensions of around 10%. The analysis of cyclic pile displacements shows that results of the different methods are in a comparable range, but differ visibly in magnitude and trend. Method-specific differences in the analysis of post-cyclic pile degradation also reveal the necessity to use elaborated cyclic design approaches with carefully selected input parameters. An exemplary sensitivity study demonstrates the distinct influence of input parameters on the results. Hence, a thorough selection of parameters based on advance static and cyclic laboratory tests (soil and possibly pile tests) as well as experience is required. Recommended tests include cyclic triaxial tests, resonant-column (RC) tests and cyclic simple shear tests.

REFERENCES

American Petroleum Institute (API) 2007. Recommended practice 2A-WSD (RP 2A-WSD), API Publishing Services.

Deutsche Gesellschaft fuer Geotechnik 2013. Recommendations on piling (EA Pfaehle), Ernst&Sohn.

Federal Maritime and Hydrographic Agency (BSH) 2012. Anwendungshinweise fuer den Standard ‚Konstruktive Ausfuehrung von Offshore-Windenergieanlagen

Fleming, K., Weltman, A., Randolph, M. and Elson, K. 2009. Piling Engineering - 3rd Edition, Taylor & Francis

Germanischer Lloyd WindEnergie GmbH (GL-Wind), 2005. Guideline for the Certification of Offshore Wind Turbines

Jardine, R., Chow, F., Overy, R. and Standing, J. 2005. ICP Design Methods for Driven Piles in Sands and Clays, Thomas Telford Publishing

Jardine, R.J., Standing, J.R.: OTO 2000 007/008 - Pile Load Testing Performed for HSE Cyclic Loading Study at Dunkirk, France; Volumes 1 & 2

Kirsch, F. 2014. Elementversuche als Baustein im Tragfaehigkeitsnachweis zyklisch belasteter Pfaehle. *Aktuelle Forschung in der Bodenmechanik 2013:* 187-205.

Kirsch, F. and Richter, T. 2012. Zyklisch belastete Offshore-Strukturen / Zum Stand der Bemessung in der Baupraxis, in 4. VDI - Fachtagung Baudynamik 2012: 553 - 568.

Kirsch, F., Richter, T. and Mittag, J., 2011. Zur Verwendung von Interaktionsdiagrammen beim Nachweis axial-zyklisch belasteter Pfaehle, *Bautechnik* 88: 319 - 324

Lueking, J. 2005. Tragverhalten von offenen Verdraengungspfählen unter Beruecksichtigung der Pfropfenbildung in nichtbindigen Boeden, *Dissertation*, Kassel Univerisity

Moormann, C. and Kempfert, H.-G. 2014. Jahresbericht 2014 des Arbeitskreises „Pfaehle“ der Deutschen Gesellschaft fuer Geotechnik (DGGT), *Bautechnik 91*, Nr. 12, Ernst und Sohn

Niazi, F.S. and Mayne, P.W. 2013. Cone Penetration Test Based Direct Methods for Evaluating Static Axial Capacity of Single Piles, *Geotechnical Geological Engineering* Nr. 31, pp. 979 - 1009,

Thomas, S. and Kempfert, H.-G. 2013. Experimentelle Erkenntnisse zum zyklisch axialen Pfahltragverhalten, *Geotechnik* 36: 169 – 178

Thomas, S. 2011. Zum Pfahltragverhalten unter zyklisch axialer Belastung, *Dissertation,* Kassel University, Germany.

Randolph, M. and Gourvenec, S. 2011. Offshore Geotechnical Engineering, Spoon Press, NY

Yu, F., Yang, J., 2012. Base Capacity of Open-Ended Steel Pipe Piles in Sand, *Journal of Geotechnical and Geoenvironmental Engineering* - ASCE, Bd. 138: 1116-1128